Kirigami pyramidal auxetic active core for wave propagation control

Manuel Collet, Morvan Ouisse, Fabrizio Scarpa, Mohamed Ichchou

ICAST2014: 25nd International Conference on Adaptive Structures and Technologies
October 6-8th, 2014, The Hague, The Netherlands

Kirigami pyramidal auxetic active core for wave propagation control

Manuel Collet [1], Morvan Ouisse [2], Fabrizio Scarpa[3], Mohammed Ichchou[1]

[1] LTDS, CNRS-Ecole Centrale de Lyon, Ecully, France
[2] FEMTO-ST, Ecole nationale de MicroMécanique, besançon, France
[3] Advanced Composites Centre for Innovation and Science (ACCIS), University of Bristol, BS8 1TR Bristol, UK

Abstract

The work describes the design and modeling of a novel pyramidal core with auxetic (negative Poisson's ratio) characteristics able to embed active distributed systems for wave propagation and vibroacoustics control. The core is made using Kirigami (Origami + cuts) techniques, which are inspired to the cutting/folding processes diffused in Asia from Japan since the 17th century. The Kirigami structure has a pyramidal unit cell shape that creates an in-plane negative Poisson's ratio behavior isotropic behavior. Mechanical analysis show that the in-plane elastic properties (Young's and shear modulus) are higher than the out-of-plane ones, a feature not observed in other centresymmetric honeycomb configurations. The core shows also evanescence patterns in 2D wave propagation analysis, even when small hysteretic damping of the core material is considered.
Tailoring the dynamical behavior of wave-guide structures can provide an efficient and physically elegant approach for optimizing mechanical components with regards to vibroacoustic propagation. Architectured materials as pyramidal core Kirigami cells and smart systems can be used to improve the vibroacoustic quality of structural components. Recently, much effort has been spent on developing new multi-functional structures integrating smart cells systems in order to optimize their vibroacoustic behavior over a larger frequency band of interest. Metacomposite concept based on shunted piezocomposites patches (MFC) glued onto periodic cores also appears as a very promising way for reaching optimal vibroacoustic functionalities.
This paper presents an integrated methodology for optimizing vibrating energy flow in interaction with pyramidal core Kirigami equipped with shunted MFC patches. The computation of the Floquet-Bloch propagators is used to optimize vibration absorption and band gap structures depending on the core design parameters and shunt impedance. We can also compare the obtained efficiency with first published realizations.

1. INTRODUCTION

Tailoring the dynamical behavior of one or two-dimensional waveguides can provide efficient and physically elegant means to optimize mechanical structures with regards to vibration and acoustic criteria, among others. However, achieving this objective may lead to different outcomes depending on the context of the optimization. In the preliminary stages of a product's development, one mainly needs optimization tools capable of rapidly providing global design directions. Such optimization will also depend on the frequency range of interest. One usually discriminates between the low frequency (LF) range and the medium frequency (MF) range, especially if vibration and noise are considered. However, it should be noted that LF optimization of vibration is more common in the literature than MF optimization. For

example, piezoelectric materials and other adaptive and smart systems are employed to improve the vibroacoustic quality of structural components, especially in the LF range (see references [Preumont 1997, Banks 1996] among many others).

Recently, much effort has been spent on developing new multi-functional structures integrating electro-mechanical systems in order to optimize their vibroacoustic behavior over a larger frequency band of interest, among which [Thorp2001] or [Collet 2009]. However, there is still a lack of studies in the literature for MF optimization of structural vibration. To that end, the aim of this study is to provide a suitable numerical tool for computing wave dispersion in two-dimensional periodic systems incorporating damping and shunted piezoelectric patches. The final aim is to allow their optimization in terms of vibroacoustic diffusion in two-dimensional waveguides. This paper is also a contribution to the challenges of designing and implementing a new class of integrated smart metacomposites capable of improved engineering performances in terms of mechanical and vibroacoustic behavior as compared to strictly passive structures.

The definition of a metacomposite combines two different aspects of vibration control. The first aspect is connected to periodic structure theories, which are usually associated with metamaterial developments. In the field of light propagation, research has explored how to design and construct photonic crystals exhibiting photonic band gaps that prevent light from propagating in certain directions with specified frequencies. Other efforts have explored creation of photonic crystals able to propagate light in anomalous and useful ways (i.e. negative refraction and artificial magnetism). In the acoustic domain, similar studies were carried out with the aim of preventing the propagation of elastic waves within a medium. For both light and acoustic waves, the band gap is obtained by periodically modulating some electromagnetic or mechanical properties [Yang 2002].

This technique presents two main problems: the spatial modulation must be of the same order as the wavelength in the gap, and the position of the band gap cannot be easily changed since it strongly depends on the materials employed (Bragg's band gap). A possible solution for these problems is found using composites with locally resonant units. The periodicity of the crystal creates a stop band that can be shifted by modifying the properties of the resonators. Liu et al. [Liu 2000] had demonstrated that a resonant sonic crystal with building blocks of rubber-coated lead balls exhibits a low-frequency sonic band gap, and the resonance can provide a maximum impedance mismatch to shield against airborne sound. The same effect can be obtained using Helmholtz resonators as showed by Fang et al. [Fang 2006, Ambati 2007] or Hu [Hu 2005]. The same idea was extended in the vibroacoustic domain for the control of elastic waves propagating into a waveguide. The resonant units in this case were obtained using RL circuits shunted to piezoelectric ceramics embedded on the structure's surface.

Numerous works have been published [Park 2005] that present analyses of the capability and efficiency of a shunted piezoelectric patch for structural damping and wave cancellation. An elegant formulation of passive shunting was first proposed by Hagood and Von Flotow [Hagood 1991] and is still commonly used. The study showed how a piezoelectric material shunted through a series RL circuit, i.e., a resonant shunt, which would exhibit a behavior analogous to the well-known mechanical tuned mass damper. Periodically induced impedance-mismatch zones generate broader stop bands, i.e., frequency bands where waves are attenuated. The tunable characteristics of shunted piezo-patches allow the equivalent mechanical impedance of the structure to be tuned so that stop bands are generated over desired frequency ranges. The presence of a resistance in the shunt circuit generates a damped resonance of the electrical network. The resistance also allows the energy dissipation mechanism of shunted piezos to be exploited, which dampens the amplitude of vibration also outside the stop bands.

The original periodic shunting concept was numerically demonstrated on rods and fluid-loaded axisymmetric shells in [Thorp 2005]. More recently, this strategy was extended to plates [Casadei 2010, Spadoni 2009, Chen 2013], where the Bloch theorem was used to predict the dispersion properties of the resulting periodic assembly. However the limitation of this approach is the narrow-band effectiveness of resonant circuits. For that reason a different circuit layout was proposed. A very effective method is based on the use of negative capacitance shunts, as originally proposed by Forward [Forward 1979]. In this

configuration, a piezoelectric patch is shunted through a passive circuit to a negative impedance converter. In this way, the internal capacitance of the piezoelectric ceramic is artificially canceled, and the impedance of the shunt circuit reduces to that of the passive circuit. Optimization of the electrical impedance for modal damping is well described in [Livet 2011]. Although the negative capacitance shunting strategy has been experimentally validated, it must be used with caution since it requires active elements that can destabilize the structure if improperly tuned. Efficiency band and stability can be improved by using specific parameters and circuit architecture [Beck 2014]. This technique requires in fact to tune the circuit very close to the stability limit [Fukada 2004, Kim 2006]. The second concept includes the definition of composite conceived in a broader sense, in which shunted piezoelectric materials, electronic components, controllers and the structure are intimately connected to each other. In this respect, the notion of programmable matter coined by Toffoli [Toffoli 1991] to refer to an ensemble of computing elements arranged in space is now extended to smart materials based on distributed piezoelectric actuators able to modify the inherent vibroacoustic properties based on an input signal. Applications of distributed shunted patchs concept on controlling vibroacoustic energy diffusion is really novative and can induced significant capacity to absorb or reflect vibration field [Tateo 2014, Tateo 2014, Collet 2014].

On the other hand, innovative manufacturing techniques have been recently applied to composites materials, like the Kirigami process. Kirigami is the ancient Japanese art of folding and cutting paper, and it has been applied to produce complex 3D cellular structures using modular moulding techniques and mathematical representation of the honeycomb lattice [Scarpa 2013], with a special topology resulting in the auxetic character of the structure. Auxetic solids have been extensively studied during the past two decades35 36. The term ‘auxetics’ indicates a wide range of mate-rials and structures exhibiting a negative Poisson’s ratio. In cellular configurations, a negative Poisson’s ratio can be achieved in re-entrant centre-symmetric (butterfly) honeycombs [Gibson 1982, Scarpa 2000], rotating rectangles and triangles [Grima 2011], as well as arrow-head [Larsen 1997] and star-shaped configurations [Grima 2005]. The centre-symmetric auxetic configuration has also been considered as a basis for gradient cellular structures [Lira 2011, Prall 1996]. All these strategies have been investigated in terms of manufacturing possibilities and mechanical performances, mainly in the static domain. However, new research activities in the areas of vibroacoustics of auxetic structures have been performed in recent years. The negative Poisson’s ratio, which provides an unusual large volume deformation during loading induces tunable wave propagation directivities not commonly observed in classical systems. Recently, some Kirigami auxetic cellular structures have also been deeply investigated in terms of wave propagation [Scarpa 2013] and the concept has been pushed toward its limits with a null Poisson’s ratio that induces negative stiffness re-gime under nonlinear deformation and high energy dissipation under cyclic loading [Virk 2013].

In this paper, the metacomposite structure of interest consists of shunted piezoelectric patches glued onto a periodical distribution of auxetic composite cells. This combinaison of both property induced by auxeticity and negative shunt circuit is analyzed in terms of modification of waves dispersion, group velocity and absorption. This controlling capability is obtained by correctly tuning the parameters of the external circuit by which almost arbitrary effective structural impedance may be obtained.

2. Piezo-Elasto Dynamical Application of the Floquet-Bloch Theorem

In this section the application of the celebrated Floquet-Bloch theorem is presented for piezo-elastodynamic problems. Based on the well-known results obtained by Floquet [Floquet 1883] for monodimensional problems and later rediscovered by Bloch [Bloch 1928] in multidimensional problems, an original application to bi-dimensional piezo-elastodynamical problem has been proposed recently [Collet 2010]. This formulation leads to very general numerical implementation for computing waves dispersion for periodically smart distributed mechanical systems incorporating electronic components,

damping effects or any frequency-dependent characteristics. The main ideas of the approach are recalled here, together with the specific points related to the inclusion of piezoelectric effects in the model.

2.1 Bloch theorem

The Bloch theorem, in its original version, gives the form of homogeneous states of Schrödinger equation with periodic potential. This theorem can be considered as a multidimensional application of the Floquet theorem [Joannopoulos, 1995]. The periodic medium (or potential) properties satisfy $M(\boldsymbol{x}+R.\boldsymbol{m})=M(\boldsymbol{x}),\ \boldsymbol{m}\in\mathbb{Z}^3$ where R is a matrice grouping the three lattice's basis vectors (in 3D). The primitive cell is defined as a convex polyhedron. The reciprocal unit cell is limited by the reciprocal lattice vector defined by the three vectors $\boldsymbol{g}_j$ so that: $\boldsymbol{r}_i.\boldsymbol{g}_j=2\pi\delta_{ij}$.

The Bloch Theorem stipulates that any function $\boldsymbol{u}(\boldsymbol{x})$ can be expressed as

$$\boldsymbol{u}(\boldsymbol{x})=\int_{\Omega_k} e^{i\boldsymbol{k}\boldsymbol{x}}\tilde{\boldsymbol{u}}(\boldsymbol{x},\boldsymbol{k})d\boldsymbol{k}$$

where the Bloch amplitude $\tilde{\boldsymbol{u}}(\boldsymbol{x},\boldsymbol{k})$ is periodic and has the representations

$$\begin{aligned}\tilde{u}(x,k)&=\sum_{n\in\mathbb{Z}^3}\hat{u}(k+Gn)e^{iGn.x},\\&=\frac{|\Omega_x|}{(2\pi)^3}\sum_{n\in\mathbb{Z}^3}u(x+Rn)e^{ik(x+Rn)}\end{aligned}$$

where $\hat{\boldsymbol{u}}(\boldsymbol{k})$ stands for the Fourier transform of $\boldsymbol{u}(\boldsymbol{x})$ and $G=[\boldsymbol{g}_1,\boldsymbol{g}_2,\boldsymbol{g}_3]$ is the reciprocal lattice matrix in the later. It can also be demonstrated that the mean value of the Bloch amplitude is the Fourier amplitude of the initial function for the corresponding wave vector. Using the Bloch theorem to represent the solutions of periodical partial derivative equations implies that all derivatives are shifted by $\boldsymbol{k}$ in the sense given by the spatial operator.

Based on that theorem, the expansion functions $\boldsymbol{v}_m(\boldsymbol{x},\boldsymbol{k})$ can be defined. They are called the Bloch eigen modes, and can be used to represent the Bloch amplitudes of any solution of the corresponding partial derivative equation as

$$\tilde{\boldsymbol{u}}(\boldsymbol{x},\boldsymbol{k})=\sum_m \boldsymbol{u}_m(\boldsymbol{k})\boldsymbol{v}_m(\boldsymbol{x},\boldsymbol{k})$$

and at the same time diagonalize the partial derivative equations. The expansion coefficients depend on the disturbance and on the induced wave vector (see [Bensoussan, 1978] for details).

2.2 Application to piezo-elastodynamic

Let us consider a piezo-elastodynamic problem made of infinite periodic distribution of unitary cell described in figure 1. The harmonic homogeneous dynamical equilibrium of system is driven by the following partial derivative equations:

$$\begin{cases}\rho\ddot{\boldsymbol{w}}(\boldsymbol{x},t)-\nabla\sigma(\boldsymbol{x},t)=0\\-\nabla D(\boldsymbol{x},t)=0\end{cases}$$

where $D(\boldsymbol{x},t)$ is the electric displacement.

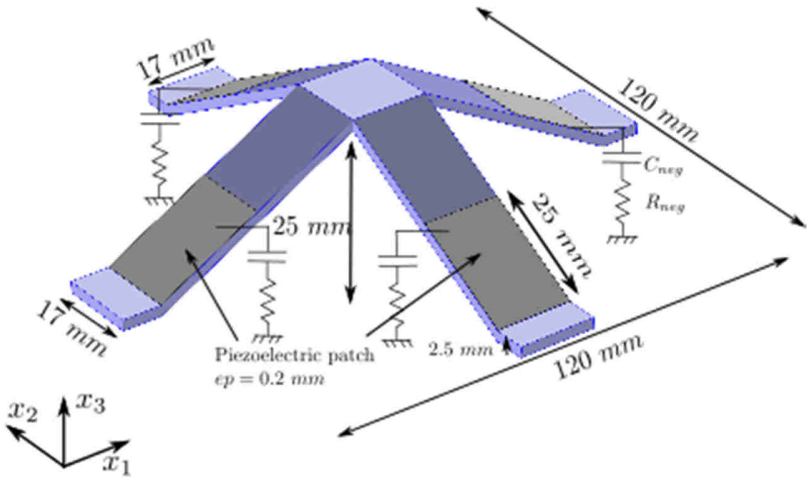

Figure 1. 3D piezocomposite periodic auxetic cell

The linear constitutive material behavior relationships can be written as

$$\sigma = C_E(\boldsymbol{x})\epsilon - e^T(\boldsymbol{x})\boldsymbol{E},$$
$$\boldsymbol{D} = e(\boldsymbol{x})\epsilon + \varepsilon_S(\boldsymbol{x})\boldsymbol{E},$$

where $\boldsymbol{E} = -\nabla V$ is the electric field vector (*V* being the voltage). We add to this set of equilibrium equations an output expression

$$q^o = -\int_{S_t} \boldsymbol{D}.\boldsymbol{n}dS$$

allowing the introduction of the charge measurement on the piezoelectric's top electrode and hence the dual counterpart of the imposed electrical Dirichlet boundary condition for applying the shunt impedance operator.

The equations above are consistent for each kind of material to the extent that null piezoelectric and permittivity tensors can be used when passive materials are considered. All of these tensors also depend on the spatial location vector and are periodic. By applying a Fourier transformation, the piezo-elastodynamic equilibrium can be rewritten in the frequency domain. As the problem is 2D infinitely periodic, mechanical boundary conditions are included in the formulation, while electrostatic boundary conditions have to be considered on each cell:

$$\begin{cases} V(\boldsymbol{x},\omega) = 0 & \forall \boldsymbol{x} \in S_b \\ V(\boldsymbol{x},\omega) = V^o(\omega) & \forall \boldsymbol{x} \in S_t \\ \boldsymbol{D}.\boldsymbol{n}(\boldsymbol{x},\omega) = 0 & \forall \boldsymbol{x} \in S_l \end{cases}$$

The top electrode applied feedback voltage depends on the shunt characteristic and on the collected charges, it can be expressed in the Fourier space by:

$$V^o(\omega) = -Z(\omega)q^o(\omega)$$

Considering a primitive cell of the periodic problem, the Bloch eigenmodes and the dispersion functions can be computed by searching the eigen solutions of the homogeneous problem with mechanical periodic boundary conditions and electric ones as:

$$\boldsymbol{u}(\boldsymbol{x}) = \begin{bmatrix} \boldsymbol{w}(\boldsymbol{x}) \\ V(\boldsymbol{x}) \end{bmatrix} = \boldsymbol{u}_{n,k}(\boldsymbol{x}) e^{i\boldsymbol{k}.\boldsymbol{x}}$$

By introducing this expression in the piezo-elastodynamic equations, $\boldsymbol{w}_{n,k}(\boldsymbol{x})$, $V_{n,k}(\boldsymbol{x})$ and $\omega_n(\boldsymbol{k})$ can be found by solving the generalized eigenvalues problem:

$$\begin{aligned} 0 = \; & \rho\omega_n^2(\boldsymbol{k})\boldsymbol{w}_{n,k}(\boldsymbol{x}) + \nabla C \nabla_{sym} \boldsymbol{w}_{n,k}(\boldsymbol{x}) + \nabla e^T \nabla V_{n,k}(\boldsymbol{x}) \\ & + ik\left[(C\nabla_{sym}\boldsymbol{w}_{n,k}(\boldsymbol{x})).\boldsymbol{\Phi} + \nabla(C\Xi_{n,k}(\boldsymbol{x}))\right] \\ & + ik\left[(\nabla e^T V_{n,k}(\boldsymbol{x})).\boldsymbol{\Phi}(e^T\nabla V_{n,k}(\boldsymbol{x})).\boldsymbol{\Phi}\right] \\ & - k^2\left[(C\Xi_{n,k}(\boldsymbol{x})).\boldsymbol{\Phi} + V_{n,k}(\boldsymbol{x})(e^T\boldsymbol{\Phi}).\boldsymbol{\Phi}\right] \forall \boldsymbol{x} \in \Omega_x, \end{aligned}$$

$$\begin{aligned} 0 \; = & -\nabla e \nabla_{sym} \boldsymbol{w}_{n,k}(\boldsymbol{x}) + \nabla \varepsilon_S \nabla V_{n,k}(\boldsymbol{x}) \\ & - ik\left[\nabla(e\Xi_{n,k}(\boldsymbol{x})) + (e\nabla_{sym}(\boldsymbol{w}_{n,k}(\boldsymbol{x}))).\boldsymbol{\Phi}\right] \\ & + ik\left[(\nabla\varepsilon_S V_{n,k}(\boldsymbol{x})).\boldsymbol{\Phi} + (\varepsilon_S\nabla V_{n,k})(\boldsymbol{x}).\boldsymbol{\Phi}\right] \\ & + k^2\left[(e\Xi_{n,k}(\boldsymbol{x})).\boldsymbol{\Phi} - (\varepsilon_S\boldsymbol{\Phi}V_{n,k}(\boldsymbol{x})).\boldsymbol{\Phi}\right] \; \forall \boldsymbol{x} \in \Omega_x, \end{aligned}$$

with

$$\begin{cases} \boldsymbol{w}_{n,k}(\boldsymbol{x} - R.\boldsymbol{m}) = \boldsymbol{w}_{n,k}(\boldsymbol{x}) & \forall \boldsymbol{x} \in S_r \; \boldsymbol{m} \in \mathbb{Z}^2, \\ V_{n,k}(\boldsymbol{x}) = 0 & \forall \boldsymbol{x} \in S_b, \\ V_{n,k}(\boldsymbol{x}) = -Z(i\omega)q^o_{n,k} & \forall \boldsymbol{x} \in S_t, \\ \boldsymbol{D}.\boldsymbol{n} = 0 & \forall \boldsymbol{x} \in S_l. \end{cases}$$

where

$$\boldsymbol{k} = k \begin{bmatrix} cos(\phi) \\ sin(\phi) \\ 0 \end{bmatrix} = k\boldsymbol{\Phi}$$

The proposed formulation is based on the computation of the Floquet vectors, instead of computing the Floquet propagators commonly used for elastodynamic applications. The full 2D waves dispersions functions can then be obtained, while damping and electrical impedance can clearly be introduced into the piezo-elastodynamic operator. The adopted methodology allows the computation of the complete complex map of the dispersion curves incorporating computation of evanescent waves and allowing the introduction of damping and shunt operator if any [Collet 2011].

2.4 Computation of the evanescence and damped power flow criteria

One aim of this paper is to provide a numerical methodology for describing particular behavior of the energy flow into the periodically auxetic structure. For doing this, we need to define a suitable indicator for distinguishing propagative and evanescent behavior especially when damped system are considered. The capability of a given Bloch wave to transport energy is given by its group velocity. Indeed, it indicates how energy is transported into the considered system and allow to distinguish the 'propagative' and 'evanescent' waves. If a Bloch eigen solution is considered, the associated group velocity vector [Maysenholder 1994] is given by

$$\boldsymbol{C}_{g_n}(\omega, \phi) = \nabla_{\boldsymbol{k}}\omega = \frac{\langle\langle \boldsymbol{S} \rangle\rangle}{\langle\langle e_{tot} \rangle\rangle} = \frac{\langle \boldsymbol{I} \rangle}{\langle E_{tot} \rangle}$$

where $\langle\langle\cdot\rangle\rangle$ is the spatial and time average respectively on one cell and one period of time, $\boldsymbol{S}$ is the density of energy flow, $\boldsymbol{I}$ the mean intensity and e_{tot}, E_{tot} the total piezomechanical energy and its time average on a period (see [Maysenholder 1994] for details).
The intensity vector is expressed as

$$\langle \boldsymbol{I}_n \rangle = -\frac{\omega}{2} Re\left(\int_{\Omega_x} C(\varepsilon_n(\boldsymbol{x}) + ik\Xi_n(\boldsymbol{x})).(\boldsymbol{w}_n^*(\boldsymbol{x})) \frac{d\Omega}{V_{ol}} \right)$$

As the spatio-temporal average of the system Lagragian is null [Maysenholder 1994], the total energy average is approximated by only computing the kinetic energy average $\langle E_{tot} \rangle$.

3. Applications for computing wave dispersion into Shunted Piezoelectric Auxetic lattice

The proposed methodology is used for the analysis of wave dispersion into the bidimensional auxetic lattice. It consists of an infinite periodic 2D waveguide made of a periodic distribution of the unitary cell presented in figure 1. The system is made of a 2.5mm thick plate assembly made of isotropic damped polymer (nu=0.4, E=30e9Pa, rho=1600kg/m^3) with a hysteretic damping factor of 0.001. The cell surface area is 120mm^2.
On all lateral branches, we add a piezoelectric patch shunted on a specific circuit made of a resistance R and a negative capacitance Cneg. These parameters are tuned to induce different wave dispersion effects and corresponding vibration behavior as explained in [Tateo 2014].
The method allows us to compute eigen frequencies corresponding to any wave vector described in cylindric coordinates system by its radius k and its angle phi in the whole first Brillouin domain. These wave numbers depending on the frequency and electric components R and Cneg.

3.1 Optimal Cneg computation

As explained in [Livet 2011] and used for experimental implementation [Tateo 2014, Collet 2014, Beck 2014], the optimal tuning for the negative capacitance term is given by the cell instability point. In fact this parameter induces a decrease in the effective cell stiffness until instability occurs. On figure 2 we show evolutions of the first eigenfrequencies of the clamped-clamped cell depending on the negative capacitance ratio alpha defined as Cneg= - alpha Co where Co=12.68nF is the effective capacitance of the glued piezoelectric patch. We observe that one eigen frequency becomes imaginary for alpha=1.64. This corresponds to the best point to tune the imaginary part of the electrical impedance [Livet 2011, Tateo 2014, Collet 2014]. Moreover the value of R allows impedance tuning in the frequency band of interest [Beck2014] and can be used to improve absorption capabilities of the metacomposite [Tateo 2014]. In the following computations we use R=0 (pure Cneg circuit) or R=500 Ohms.

3.2 Dispersion along Gamma-X direction of the system

The wave's dispersion curves of the system along the Gamma-X direction are plotted on Figure 3 for closed circuit, pure Cneg circuit and R-Cneg configuration. This figure shows the real part the dispersion curves of propagative modes. The evanescent waves was filtered by using criterion based on the ratio between the real and imaginary parts of the obtained complex wave numbers. The obtained results indicate a deep complexity of the vibroacoustic behavior of the studied system with a first band gap between 2300 and 3200Hz.

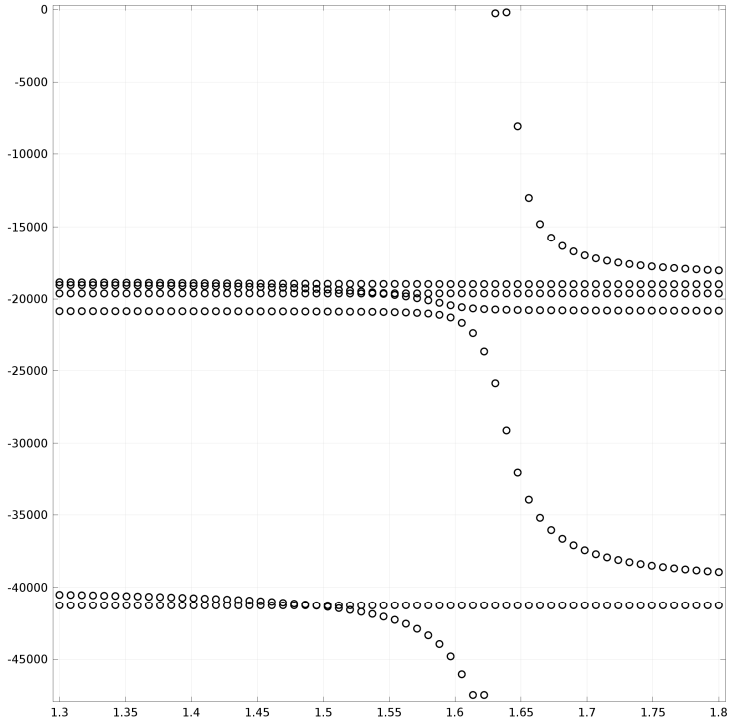

Figure 2. Eigenfrequencies of clamped-clamped cell as a function of the negative capacitance ratio alpha

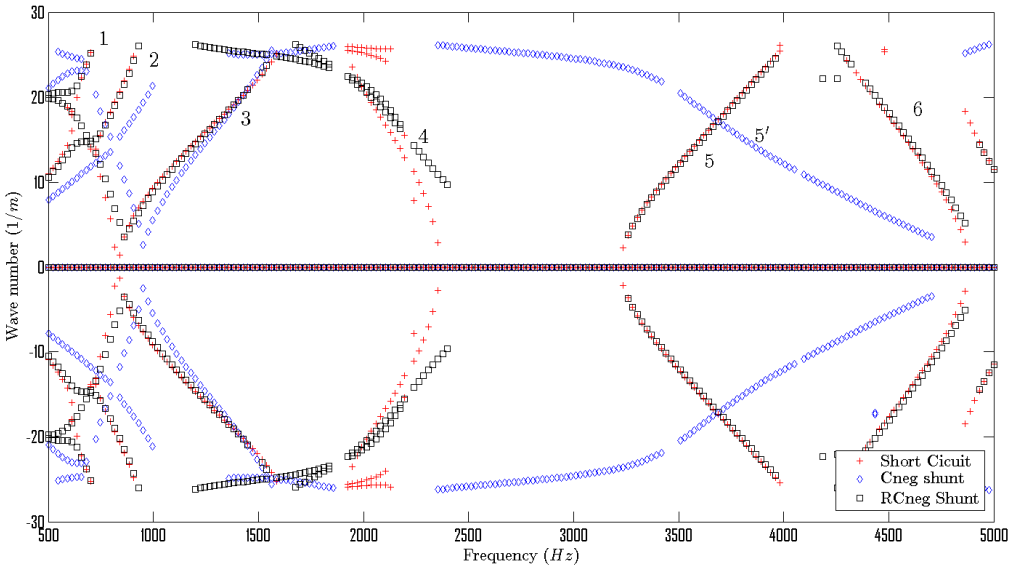

Figure 3. Dispersion curves of propagative modes of the system

All modes corresponding to each principal branches numbered 1 to 6 on the figure 3 are given on figures 4 and 5.

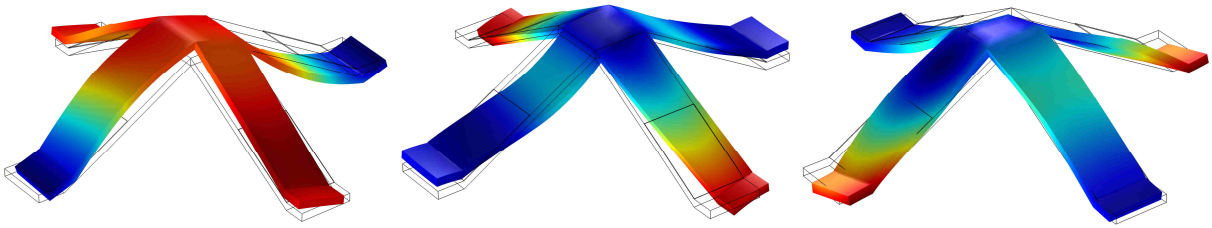

Figure 4. Mode shapes of branches 1, 2 and 3

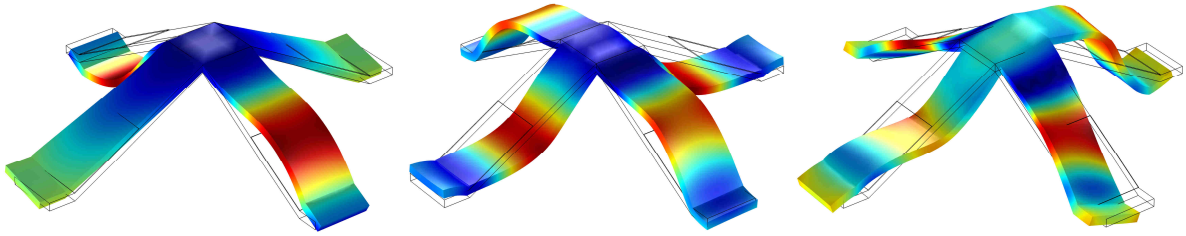

Figure 5. Mode shapes of branches 4, 5 and 6

We underline that:

- the pure Cneg circuit tends to increase wave phase velocity and modify location and size of the band gap;
- the RCneg circuit does not induce strong modifications of the dispersion curves;
- the new Cneg branch 5' crossing the initial band gap corresponds to a mode shape totally different than branch 5 existing with short circuit (see figure 6). The Cneg shunt cancels propagation of branch 5 and strongly modify those of branch 4. In this sense, the shunt enlarge the initial band gap.

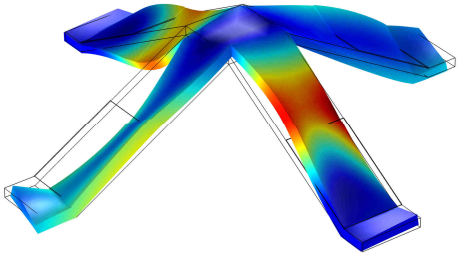

Figure 6. Mode shape of branch 5' created by pure Cneg shunt

The wave's imaginary part of dispersions curves along the Gamma-X direction are plotted on Figure 7. We can point out that the RCneg circuit greatly improves the damping on branches 1, 2, 3 while the increase on branches 4, 5 and 6 is smaller than the one obtained in the pure Cneg configuration. The pure Cneg circuit creates a strongly damped new branch 5' and modifies all the dispersion properties in the higher frequencies.

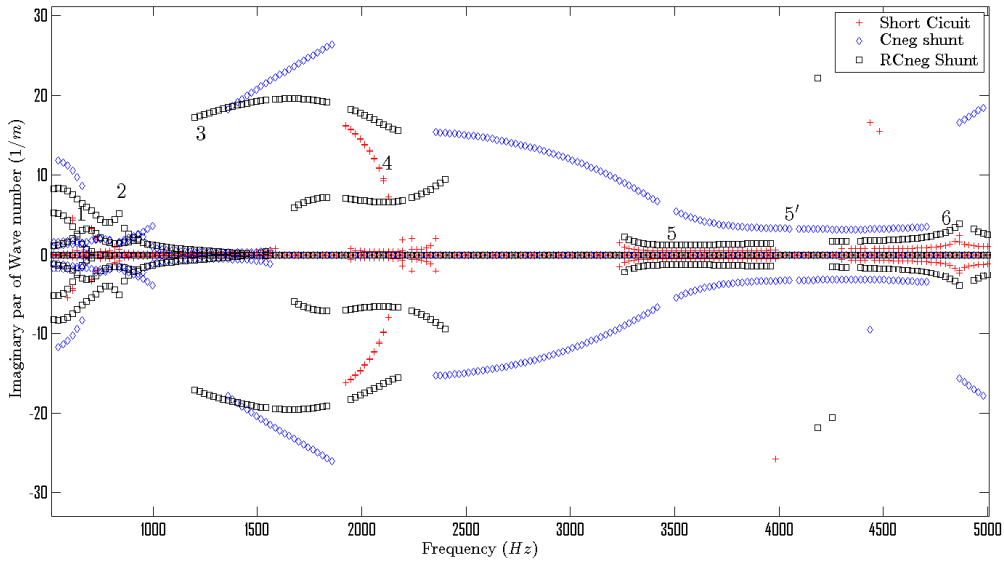

Figure 7. Imaginary Dispersion curves of propagative modes of the studied system

4 Concluding remarks

The kirigami pyramidal auxetic active core described in this work has shown the following characteristics:

(1) The lattice has an in-plane auxetic behavior, with values of the negative Poisson's ratio depending on the geometry parameters of the cellular configurations. The lattice includes shunted piezoelectric elements.

(2) The shunt circuit is constituted by a negative capacitance and a resistor. The value of the capacitance has been optimized using stability limit considerations. Pure negative capacitance shunt and resistance/negative capacitance shunt have been compared to the short circuit configuration.

(3) The pure Cneg circuit tends to increase wave phase velocity and modify location and size of the band gap; it creates a strongly damped new branch and modifies all the dispersion properties in the higher frequency range. An effect of band gap enlargement has been observed.

(4) The RCneg circuit does not induce strong modifications of the dispersion curves; but greatly improves the damping on branches 1, 2, 3 while the increase on branches 4, 5 and 6 is smaller than the one obtained in the pure Cneg configuration.

ACKNOWLEDGMENTS

This study is a collaborative effort supported by the FrenchResearch Agency (CALIOP Project grant number NT09-617542 and Labex Action grant number ANR-11-LABX-0001-01).

REFERENCES

1. Alderson A; Alderson KL (2007). Proc. Inst. Mech. Eng. G 221
2. Ambati, M., Fang, N., Sun, C., Zhang, X., 2007. Surface resonant states and superlensing in acoustic metamaterials. Physical Review B 75 (19), 195447.
3. Banks, H., R.C. Smith, Y. W., 1996. Smart material structures Modeling Estimation and Control. Masson and Wiley.
4. Beck, B. S., Cunefare, K. A., Collet, M., 2014. Response-based tuning of a capacitance shunt for vibration control. Journal of Intelligent Material Systems and Structures 25, 1585–1595.
5. Bensoussan, A., Lions, J., Pananicolaou, G., 1978. Asymptotic Analysis for Periodic Structures. North Holland.
6. Bloch, F., 1928. Über die Quantenmechanik der Electron in Kristallgittern. Zeitschrift für Physik 52, 550–600.
7. Casadei, F., Ruzzene, M., Dozio, L., Cunefare, K., 2010. Broadband vibration control through periodic arrays of resonant shunts: experimental investigation on plates. Smart Materials and Structures 19 (1), 150.
8. Chen, S., Wang, G., Wen, J., Wen, X., 2013. Wave propagation and attenuation in plates with periodic arrays of shunted piezo-patches. Journal of Sound and Vibration 332 (6), 1520–1532.
9. Collet, M., Cunefare, K., Ichchou, N., 2009. Wave Motion Optimization in Periodically Distributed Shunted Piezocomposite Beam Structures. Journal of Int Mat Syst and Struct 20 (7), 787–808.
10. Collet, M., Ouisse, M., Ichchou, M., 2012. Structural energy flow optimization through adaptive shunted piezoelectric metacomposites. Journal of Intelligent Material Systems and Structures 23 (15), 1661–1677.
11. Collet, M., Ouisse, M., Tateo, F., 2014. Adaptive metacomposites for vibroacoustic control applications,. IEEE Sensors Journal 14 (7), 2145–2152.
12. Fang, N., Xi, D., Xu, J., Ambati, M., Srituravanich, W., Sun, C., Zhang, X., 2006.
13. Ultrasonic metamaterials with negative modulus. Nature Materials 5 (6), 452–456.
14. Floquet, G., 1883. Sur les équations différentielles linéaires à coefficients périodiques. Annales de l'Ecole Normale Supérieure 12, 47–88.
15. Forward, R., 1979. Electronic damping of vibrations in optical structures. Applied Optics 18 (5), 690–697.
16. Fukada, E., Date, M., Kimura, K., Okubo, T., Kodama, H., Mokry, P., Yamamoto, K., 2004. Sound isolation by piezoelectric polymer films connected to negative capacitance circuits. IEEE Transactions on Dielectrics and Electrical Insulation 11 (2), 328–333.
17. Gibson L J, Ashby M F, Schajer G S, Robertson C I (1982). Proc. R. Soc. 382
18. Grima J N, Alderson A, Gatt R, Evans K E (2005). Mol. Simul. 31
19. Grima J N, Manicaro E and Attard D (2011) Proc. R. Soc. A 467
20. Hagood, N., von Flotow, A., 1991. Damping of structural vibrations with piezoelectric materials and passive electrical networks. Journal of Sound and Vibration 146 (2), 243–268.
21. Hu, X., Chan, C., Zi, J., 2005. Two-dimensional sonic crystals with helmholtz resonators. Physical Review E 71 (5), 556.
22. Joannopoulos, J., Meade, R., Winn, J., 1995. Photonic Crystals: Molding the Flow of Light. Princeton University Press.
23. Kim, J., Jung, Y., 2006. Broadband noise reduction of piezoelectric smart panel featuring negative-capacitive-converter shunt circuit. The Journal of the Acoustical Society of America 120 (4), 2017–2025.
24. Kittel, C., 1986. Introduction to Solid State Physics. John Wiley and Sons, New York.
25. Larsen D U, Sigmund O, Bouwstra S (1997) IEEE J. Microelectromech. Syst. 6
26. Lehoucq, R., Sorensen, D., Yang, C., 1998. ARPACK users' guide: solution of largescale eigenvalue problems with implicitly restarted Arnoldi methods. Siam.

27. Lira C, Scarpa F, Rajasekaran R (2011) J. Intell. Mater. Syst. Struct. 22
28. Liu, Z., Zhang, X., Mao, Y., Zhu, Y., Yang, Z., Chan, C., Sheng, P., 2000. Locally resonant sonic materials. Science 289 (5485), 1734–1736.
29. Livet, S., Collet, M., Berthillier, M., Jean, P., Cote, J., 2011. Structural multi-modal damping by optimizing shunted piezoelectric transducers. European Journal of Computational Mechanics 20 (1-4), 73–102.
30. Lorato A, Innocenti P, Scarpa F, Alderson A, Alderson K L, Zied K M, Ravirala N, Miller W, Smith C W, Evans K E (2010). Compos. Sci. Tech-nol. 70.
31. Nelson, S., 1992. Active Control of Sound. Pub. Academic Press, London, San Diego.
32. Park, C., Baz, A., 2005. Vibration control of beams with negative capacitive shunting of interdigital electrode piezoceramics. Journal of Vibration and Control 11 (3), 331–346.
33. Prall D, Lakes RS (1996) Int. J. Mech. Sci. 39
34. Preumont, A., 1997. Vibration control of structures : An introduction. Kluwer.
35. Scarpa F, Panayiotou P, Tomlinson G (2000) J. Strain Anal. Eng. Des. 35
36. Scarpa, F; Ouisse, M; Collet, M; Saito, K (2013) ASME Journal of Vibration and Acoustics 135(4)
37. Schenk, O., Gärtner, K., 2004. Solving unsymmetric sparse systems of linear equations with PARDISO. Future Generation Computer Systems 20 (3), 475–487.
38. Spadoni, A., Ruzzene, M., Cunefare, K., 2009. Vibration and wave propagation control of plates with periodic arrays of shunted piezoelectric patches. Journal of Intelligent Material Systems and Structures 20 (8), 979–990.
39. Tateo, F., Collet, M., Ouisse, M., Cunefare, K., 2014a. Design variables for optimizing adaptive metacomposite made of shunted piezoelectric patches distribution. Journal of Vibration and Control, 1077546314545100.
40. Tateo, F., Collet, M., Ouisse, M., Ichchou, M., Cunefare, K., Abbe, P., 2014b. Experimental characterization of a bi-dimensional array of negative capacitance piezopatches for vibroacoustic control. Journal of Intelligent Material Systems and Structures 21, 1045389X14536006.
41. Thorp, O., Ruzzene, M., Baz, A., 2001. Attenuation and localization of wave propagation in rods with periodic shunted piezoelectric patches. Proceedings of SPIE – The International Society for Optical Engineering Smart Structures and Materials 4331, 218–238.
42. Thorp, O., Ruzzene, M., Baz, A., 2005. Attenuation of wave propagation in fluidloaded shells with periodic shunted piezoelectric rings. Smart Materials and Structures 14 (4), 594.
43. Toffoli, T., Margolus, N., 1991. Programmable matter: Concepts and realization. Physica D: Nonlinear Phenomena 47 (1-2), 263–272.
44. Virk, K; Monti, A; Trehard, T; Marsh, M; Hazra, K; Boba, K; Remillat, CDL; Scarpa, F; Farrow, IR (2013). Smart Materials and Structures 22(8)
45. Yang, S., Page, J., Liu, Z., Cowan, M., Chan, C., Sheng, P., 2002. Ultrasound tunneling through 3D phononic crystals. Physical Review Letters 88 (10), 104301.